Proceedings of IMECE'03
2003 ASME International Mechanical Engineering Congress and Exposition
Washington, D.C., November 16-21, 2003

ICEME2003-42313

Investigation of White Layers Formed in Conventional and Cryogenic Hard Turning of Steels

Zbigniew Zurecki, Ranajit Ghosh, and John H. Frey
Air Products & Chemicals, Inc.
Allentown, PA 18195

ABSTRACT

Although hard turning of steels has become an accepted industrial practice reducing the extent of grinding, many surface integrity aspects of hard turning require clarification. The striking result of hard turning is the tendency for forming white (non-etching) and dark (overtempered) layers at machined surface. White layers are often associated with residual tensile stresses leading to reduced fatigue strength and poor wear resistance. It has been reported that certain steel compositions, machining conditions, and tools enhance white layers, but no consensus was reached on the nature of white layer and the role of environmental factors. This study examines the impact of cryogenic, liquid nitrogen spray cooling, tool and work materials, as well as machining speed on white layer formation. Results are evaluated using XRD, SEM, EDS, AES, residual stress measurement and microhardness profiling. It is concluded that white layers are a purely thermomechanical phenomenon involving dissolution of low-alloy carbides into austenitic matrix, and catastrophic flow of that 1-phase material resulting in its nano-scale refinement. The depth and extent of the refinement are controlled by cooling, with the cryogenic nitrogen reducing white layer thickness, loss of hardness, and improving residual stress distribution.

INTRODUCTION

Hard turning, or lathe turning of steel parts heat-treated to the hardness exceeding 50-55 HRC, is gradually gaining popularity in the manufacturing industries due to the reduction of capital, operating, and environmental compliance costs involved in the conventional, surface grinding operations it replaces. Like in the case of grinding, depending on machining parameters and work material, hard turned surfaces reveal a thermomechanical defect termed "white layer" for its resistance to metallographic etching. Since grinding defects are known to introduce tensile stresses, reduce fatigue strength and surface hardness [1-3], considerable industrial and academic attention has been given to the mechanical evaluation of hard turned parts containing white layers [4-11]. Recently, the use of aggressive machining conditions has been proposed for grinding and hard turning operations to harness the white layer related transformations and combine material shaping with an *in-situ* surface hardening [12-13]. Although the structure of hard turned white layer, the fundamental mechanisms responsible for its formation, and its impact on engineering properties continue to be a subject of debate, there is a reasonable consensus that an increase in the thermomechanical energy dissipated at the work-tool contact area leads to an undesired enhancement and tensile stressing of white layer. The increase can result from the use of a less sharp and/or worn tool, more negative tool geometries, higher machining speeds and feedrates, [4, 6, 8,10, 13-20] as well as higher depths of cut [21], since typical hard turning processes generate relatively large radial cutting forces [22]. Removal of the heat from the contact area, the other side of the energy management problem, received only a scant attention. As Park [23], Dawson and Kurfess [24] noted, low conductivity tools such as alumina ceramics or "low-content" CBN generate thicker, less desirable white layer than their "high-content" CBN counterparts. Similar observations were made, earlier, in the case of grinding [2,4]. However, the convective cooling effect of cutting fluids on hard turning white layer has not been clarified [8]. Konig [25] suggested suppression of white layers with coolants but the others [6-7] indicated no effect. The problem of heat removal has been mute for several reasons: (a) low-content-CBN tools can live longer during hard turning than the high-content CBN [26], (b) both CBN tool types are preferred over alumina in dry machining, (c) the tool-life considerations discourage the use of the conventional cutting fluids with low-content CBN [22], the use of the fluid with alumina tools results in accelerated tool fractures [27], and the environmental advantages of hard turning as a replacement for grinding, diminish with the use of fluids.

A new, environmentally acceptable and highly effective cooling method has been developed in the recent years on an industrial scale which involves spraying of the rake of cutting inserts with a small quantity of rapidly vaporizing cryogenic liquid nitrogen [28-29]. Cryogenic machining reports indicate marked process improvements during cutting of Ti-6Al-4V, mild and soft steels as well as hard, Si_3N_4 workpieces [30-40]. Recent research and industrial applications show that the cryogenic spray machining results in a significant enhancement of the life of alumina and CBN tools during hard turning which enables the use of higher material removal rates than during the conventional hard turning [41]. Since the economic benefits of a high-speed hard turning, especially with inexpensive alumina tools, can be critical for finishing operations, the primary objective of the present study is to explore effect of (*i*) cryogenic coolant and (*ii*) alumina tool on white layer. Additional objective includes microstructural examination of transformation events leading to white layers.

EXPERIMENTAL

Popular bearing steel, AISI 52100, has been selected for the main portion of the present hard turning study. Disks made of that steel, sized 3.75-inch (95 mm) dia., were oil quenched and low-tempered to the target hardness of 60 HRC. Two types of cutting tools were used in hard turning: a "low-content" cubic boron nitride (CBN) and an alumina-based, black ceramic (Al_2O_3). Due to commercial availability, the CBN inserts had a slightly narrower chamfer than the Al_2O_3 inserts which could affect machining dynamics and thermomechanical effects on work material. The tools were used without coolant, in a dry machining mode, and with a liquid nitrogen cooling jet (LIN) spraying at their rake surfaces. Two cutting speeds were used with each tool and each cooling condition, 400 ft/min. (122 m/min.) and 700 ft/min. (213 m/min.); the depth of cut and feedrate were kept constant. Hard turning tests were carried out in a facing mode on a 20kW CNC lathe. Each disk was machined with a new, sharp tool. One set of face-hard turned disks was used for residual stress measurement by hole-drilling method, ASTM Std E837. Hard turned disks from the other set were sectioned into samples as shown on Fig.1. A part of the samples was used for microstructural examination, and another part was subject to post-machining heat-treatments before final examination. The elected geometry of test disks and face cutting assured uniformity of hard turned material in view of limited hardenability of AISI 52100 steels. Moreover, the residual stress measurement did not require prior sectioning of test coupons, i.e. has not resulted in an uncontrolled stress relieving. AISI A2 tool steel has been selected as an additional work material of this study. Disk preparation, hard turning, and metallographic sample cutting procedure used with A2 were the same as in the case of 52100 steel. Table 1 details experimental data and procedures used.

Table 1: Testing and Analytical Procedures

1. Cutting tools	Cutting insert:	"Low-content PCBN" type, CBN-TiN	Al_2O_3-TiCN "black" type ceramic
	Insert description:	BNC80, 4NC-CNMA432, 4 cutting edges, PVD-TiN coated,	KY4400, CNGA432, 4 cutting edges, PVD-TiN coated,
	Edge chamfer angle, measured:	25^o +/- 3^o	25^o +/- 3^o
	Chamfer width, measured:	0.0035 inches (0.09 mm)	0.0045 inches (0.11 mm)
	Toolholder's angles:	-5^o rake angle and –5^o inclination angle	same
2. Cutting parameters	Cutting speeds in feet/minute:	400 and 700 (122 and 213 m/min., respectively)	
	Feedrate in inches/revolution:	0.004 (0.102 mm)	
	Depth of cut in inches:	0.015 (0.381 mm)	
	Cutting (feeding) direction:	Radial (along X-axis), facing operation	
3. Cooling conditions	Cooling methods used during machining:	[1] Dry (no cooling, ambient air convection), and [2] LIN – a boiling liquid nitrogen jet at -197 ^{o}C discharged at the insert rake from the pressure of 100 psig (0.69 MPa), total jet mass flowrate of 12 g/s, 2-phase: 90 vol% liquid and 10 vol% gas phase	
4. Workpiece material tested	AISI 52100 bearing steel, 1.0wt% carbon, 1.5wt% chromium	Austenitized in 1% carbon-potential atmosphere, then, oil quenched and low-tempered to 60 HRC +/- 2 HRC	
5. White layer examination conditions	Material volume removed by new cutting edge and number of interruptions before sampling of machined surface for white layer:	1.1 cubic inches including 8 cutting interruptions (18 cm^3)	
	Residual stress measurement method:	Incremental hole drilling with 1 mm diameter drill, extensometer rosette, per ASTM E837	
	Direction of metallographic cut for image evaluation and microhardness measurements:	Perpendicular to as-machined workpiece surface and in the radial direction (along X-axis), see sketch below.	
	Microhardness measurement method – Knoop, 100G load applied for 15 seconds	Profiling hardness as a function of depth under as-machined workpiece surface with blade-shaped indenter	
	Etchant developing white layer contrast:	Nital – 5%HNO_3 in ethanol applied to sample surface for 10 seconds	
	Microanalytical techniques used:	SEM – scanning electron microscopy, secondary image, 15kV accel. volt. EDS (EDX) – energy dispersive X-ray spectroscopy, 15kV accel. volt. AES – Auger electron spectroscopy, field emission scanning nanoprobe, 10keV - 1.1 min., 10-min. sputtering to remove carbon contaminants from analyzed surface, XRD – X-ray diffraction, 0.5-5.0 glancing angles with 24 hrs scans plus std 30-90 degree with 1hr scans	
6. Heat treatments of selected samples after machining	Dry and LIN 52100 samples previously machined with the Al_2O_3 cutting insert and confirmed to contain white layer	[1] high-tempering tempering – 565^{o}C in pure argon atmosphere. [2] austenitizing – 1010^{o}C in pure argon atmosphere, slow cooled.	
7. Additional workpiece material	AISI A2 tool steel, 1.0wt% carbon, 5wt% chromium, 1wt% molybdenum	Air quenched and low-tempered to 61 HRC +/- 1 HRC	

RESULTS

All 52100 samples revealed the presence of thin white and dark layers following hard turning as shown on Fig.2. The thickness of white layers scaled with the cutting speed and was markedly reduced by the use of LIN cooling, Fig.3. The effect of tool material was more complex; alumina tools produced thinner white layers at the lower cutting speed than CBN, and the trend reversed at the higher cutting speed. Considering a low thermal conductivity alumina, both these observations indicate the key effect of the contact temperature on white layer thickness. No white and dark layers were observed on the A2 samples which retained a virtually intact microstructure, even though the thermomechanical energy dissipated at the A2 work surface must have been quite similar to the energy in the 52100 tests. Thus, the observed difference may be explained by a higher thermal stability of alloyed carbides and matrix of the heat-treated A2 steel.

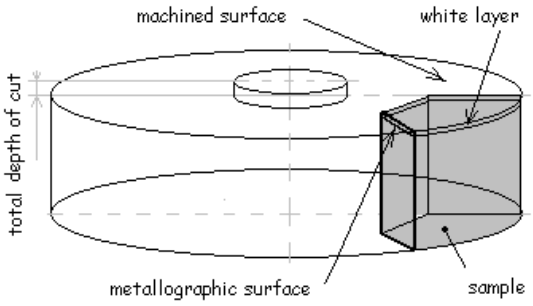

As-machined surface roughness, Ra, micro-inches, at cutting speed of 700 ft/min.

CBN-Dry	CBN-LIN	Al2O3-Dry	Al2O3-LIN
17	15	26	14

Fig.1: Method of machining and cutting test samples. [17μinch= 0.43μm, 15μinch=0.38μm, 26μinch=1.0μm and 14μinch= 0.35μm]

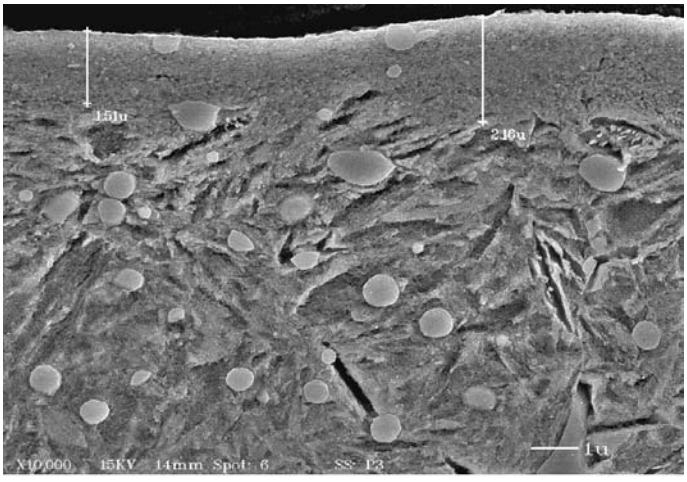

Fig.2: Cross-section of white (top) and dark (bottom) layer, a typical microstructure of hard turned steel 52100 showing carbides dissolving within white layer, SEM, orig. magnif. x 10,000, a light Nital etching.

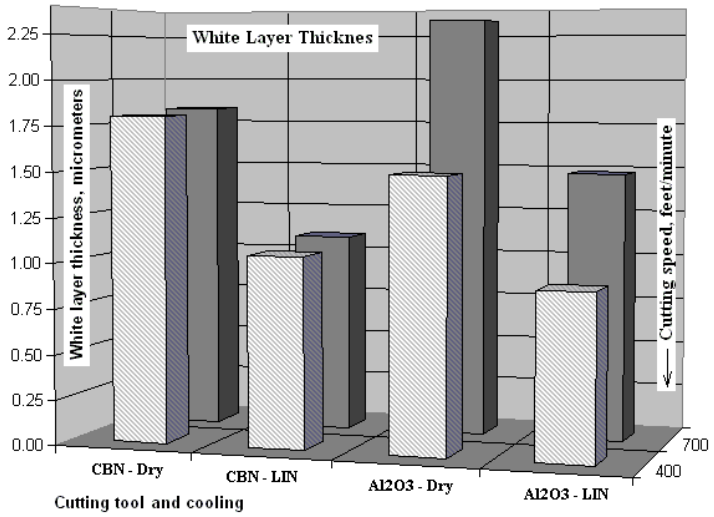

Fig.3: Results of SEM image-based white layer measurements on samples hard turned at the speed of 400 and 700 ft/min (122 and 213 m/min., respectively). Not shown, the average thickness of dark layer was about 50 μm for LIN-cooled tools and 100 μm for dry-machining tools regardless of tool material used, CBN or Al_2O_3.

Figure 4 shows EDS spectrum of a 1 μm-sized, low-Cr carbide located at the interface between an apparently homogenous white layer and the overtempered martensite dark layer of the 52100 samples. Such "microscopic" carbides largely dissolve within the white layer to form a nanocrystalline, cell structure, Fig.5. Interestingly, the nanocrystalline cells are significantly larger in the case of LIN machining, indicating that the degree of carbide dissolution and refinement is a strong function of local temperature. Mechanical consequences of hard turning without cooling include surface softening, Fig.6, and uneven, more fluctuating residual stresses, Fig.7. In contrast, LIN cooling of the tool and the contact area resulted in the retention of the parent metal's hardness, flatter stress gradients, and elimination of tensile stresses in the case of hard turning with alumina inserts. AES maps of C, O, and Fe distributions within the white and dark layers confirm the carbide dissolution hypothesis and the absence of interfacial reaction products with machining environment. This result is not unexpected since, at least in the case of dry hard turning, it would be quite difficult to enrich a relatively thin white layer in carbon and, at the same time, oxidize it without reducing carbon level and/or forming a film of oxide. A series of XRD scans on hard turned surfaces detected a thin, nanocrystalline layer comprising ferrite and carbides, as well as some martensite and retained austenite, the secondary phases, Fig.9 and 10. A composite sketch with XRD results shows that the fraction of martensite and austenite becomes more significant only under the white layer, within the overtempered dark layer. Thus, in contrast to the hard turning references [6-7,9,15,18], the white layer analyzed in this work cannot be described either as a quenched, brittle martensite, or an austenite.

High thermal sensitivity of white and dark layers is elucidated further by results of post-hard turning heat-treatments in inert atmosphere, Fig.11, and chip examination, Fig.12. Tempering just as

well as austenitizing of the hard turned, 52100 samples restores the conventional structures expected for a tempered or annealed material and provides no evidence of surface reaction products. The white areas of segmented chips, presumably cooling faster than the surface of hard turned workpiece, show a nanocrystalline, cell structure only in the case of dry machining and a coarser, temper structure with submicron carbides after LIN machining. The impact of cooling rate, limiting structural refinement and carbide dissolution effects is evident. Surface of the alumina insert used dry at 700 ft/min (213 m/min) shows signs of an interparticle melting, Fig.13, probably a result of high-temperature reaction between the chip and the Al_2O_3-TiCN tool materials. The effect coincides with the thickest white layer measured in this study, see Fig.3. Melting of TiCN ceramics during dry sliding against steel at the speed of only 630 ft/min (192 m/min) was reported by Xingzhong et al. [42].

DISCUSSION

The following sequence of events leading to the white layer formation emerges from the presented data. (*I*) The thermal input and plastic shearing of work surface result in a spike of temperature, an extensive microstructural refinement, and a nearly complete dissolution of carbides in the surface layer.

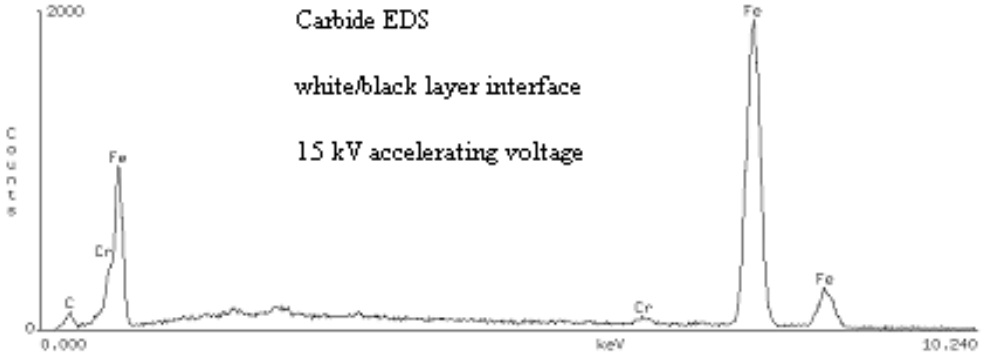

Fig.4: EDS spectrum of a 1 μm sized carbide found within the interface between white and dark layer; the presence of chromium in the Fe-C carbide is evident.

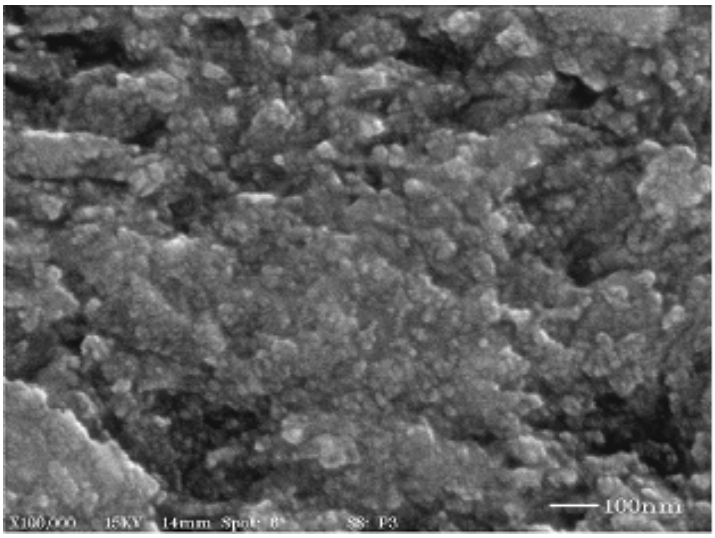

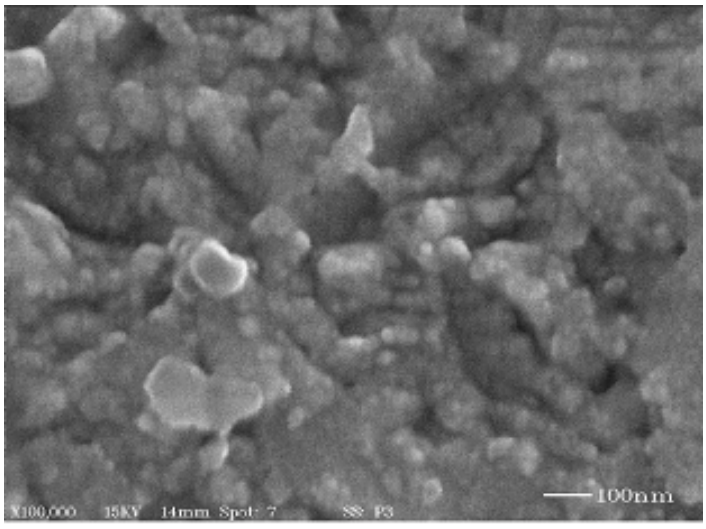

Fig.5: Close-up view of white layers produced during hard turning of the 52100 steel with Al_2O_3 tool shows a nanocrystalline, cellular structure; SEM, orig. magnif. x 100,000. (Left) dry hard turning, average cell size - 20 nm. (Right) LIN hard turning, average cell size - 80 nm, i.e. significantly coarser than in the case of dry hard turning.

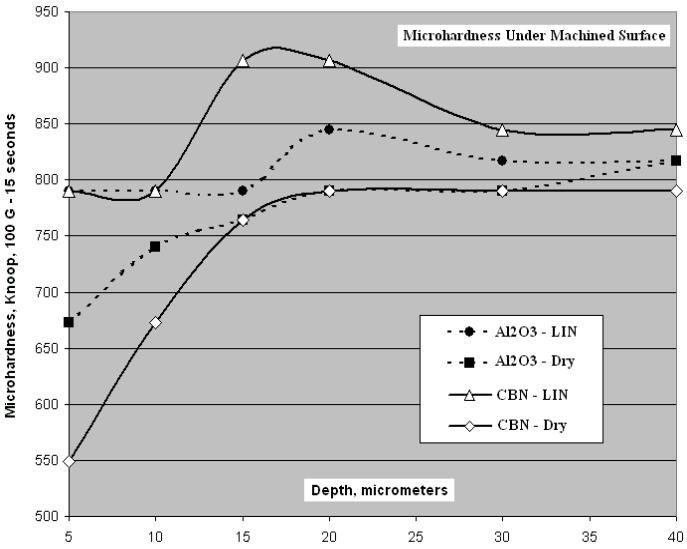

Fig.6: Knoop microhardness profile as a function of depth under machined surface, multipoint averages. Significant loss of subsurface hardness is evident in the case of dry machining.

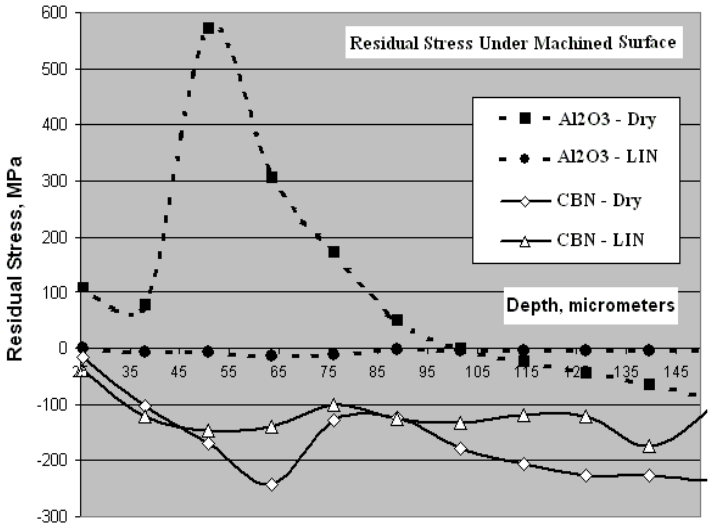

Fig.7: Residual stress as a function of depth under machined surface, radial sample direction (across turning lines). Note a more uniform and neutral-to-compressive stress in the case of LIN hard turning.

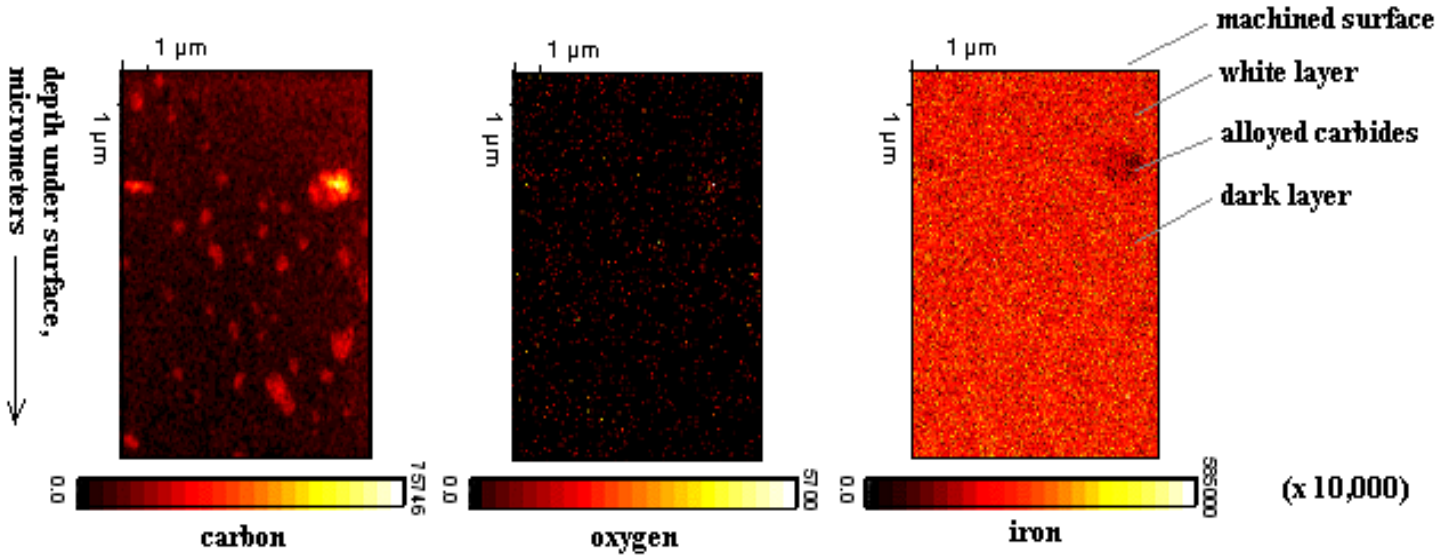

Fig.8: AES elemental distribution map for the white (top) and dark (bottom) layer cross-section examined at the magnification of 10,000 times. The white layer material is homogenous and enriched with carbon; the oxygen and nitrogen levels were low and uniform across the entire analyzed area.

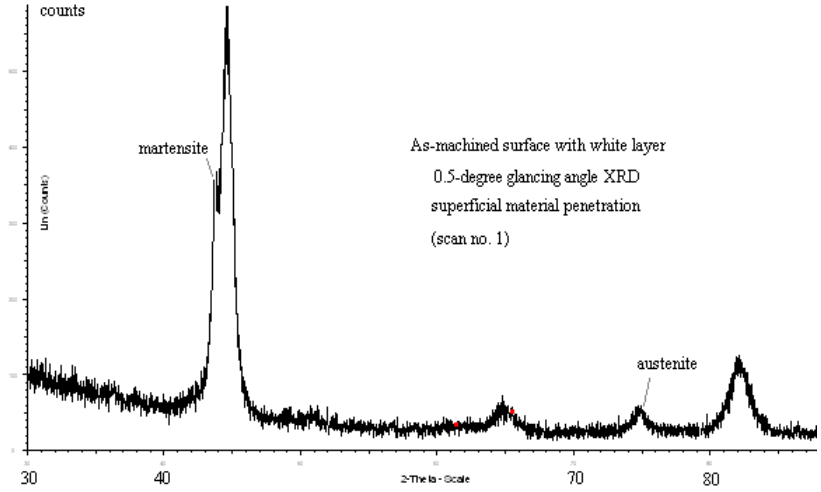

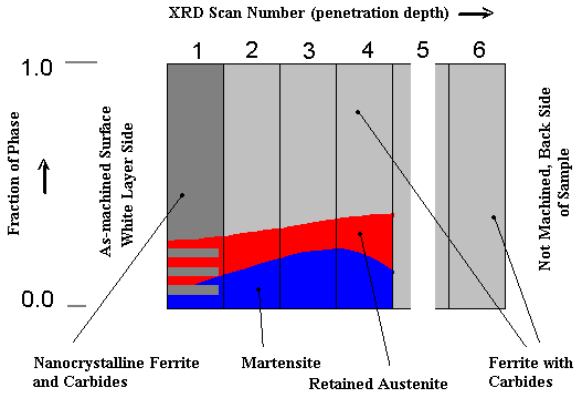

Fig.9 (left): An example of XRD spectra obtained from as-machined surface. Martensite and austenite peaks were secondary, and the main phases of white layer couldn't be identified using standard spectra libraries. Line broadening indicates nanocrystalline structure.

Fig.10 (right): A composite map of phase distribution in white and dark layer summarizing results of multiple XRD scans with increasing glancing angles. White layer consists of nanocrystalline ferrite and carbides with weak peaks of martensite and austenite. Located deeper, dark layer is characterized by an increasing level martensite and retained austenite in a normally-sized ferrite/carbide matrix. The spectrum of the unaffected portion of sample material is typical for tempered steels with tempered ferrite and carbides.

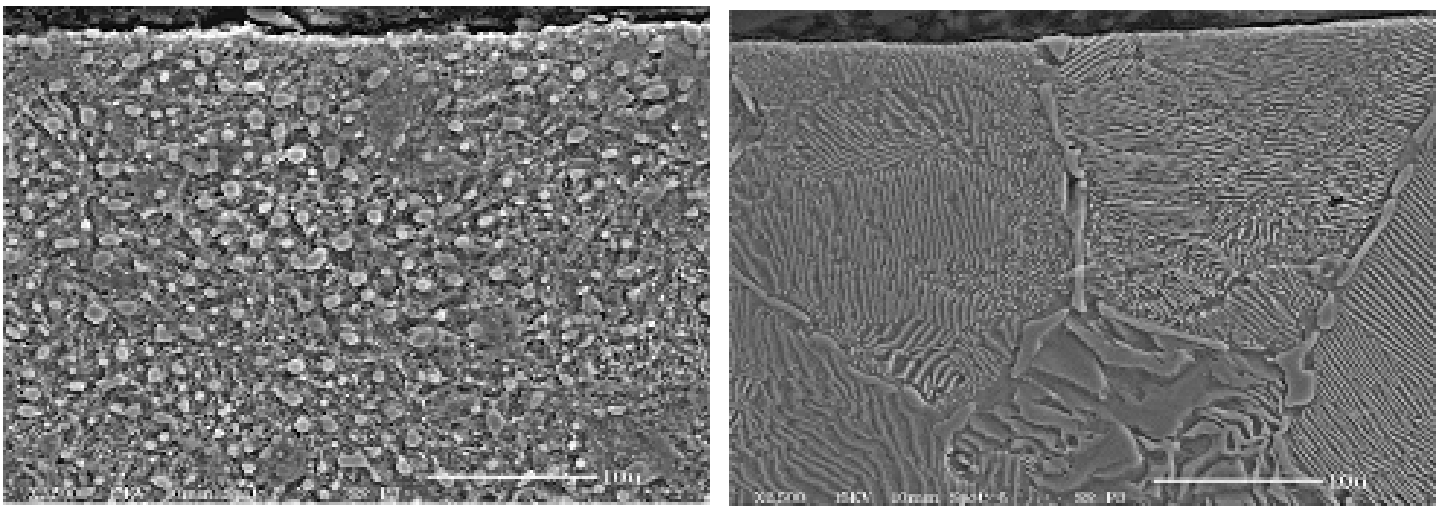

Fig.11: Cross-section through the machined surface of the white layer-containing samples subjected to heat treatments following the hard turning step, SEM, orig. magnif. x 3,500, a light Nital etching. (Left) Tempered under argon at 565^{o}C and (right) austenitized under argon at 1010^{o}C. Both treatments resulted in a complete dissolution of white and dark layer structures. As expected, the tempered structure contains uniformly distributed carbides in a fine-grained, post-martensitic ferrite, and the austenitized structure is pearlitic with carbide plates at the located at the grain boundaries of former austenite. No evidence of a chemically modified surface layer was observed at the machined surface.

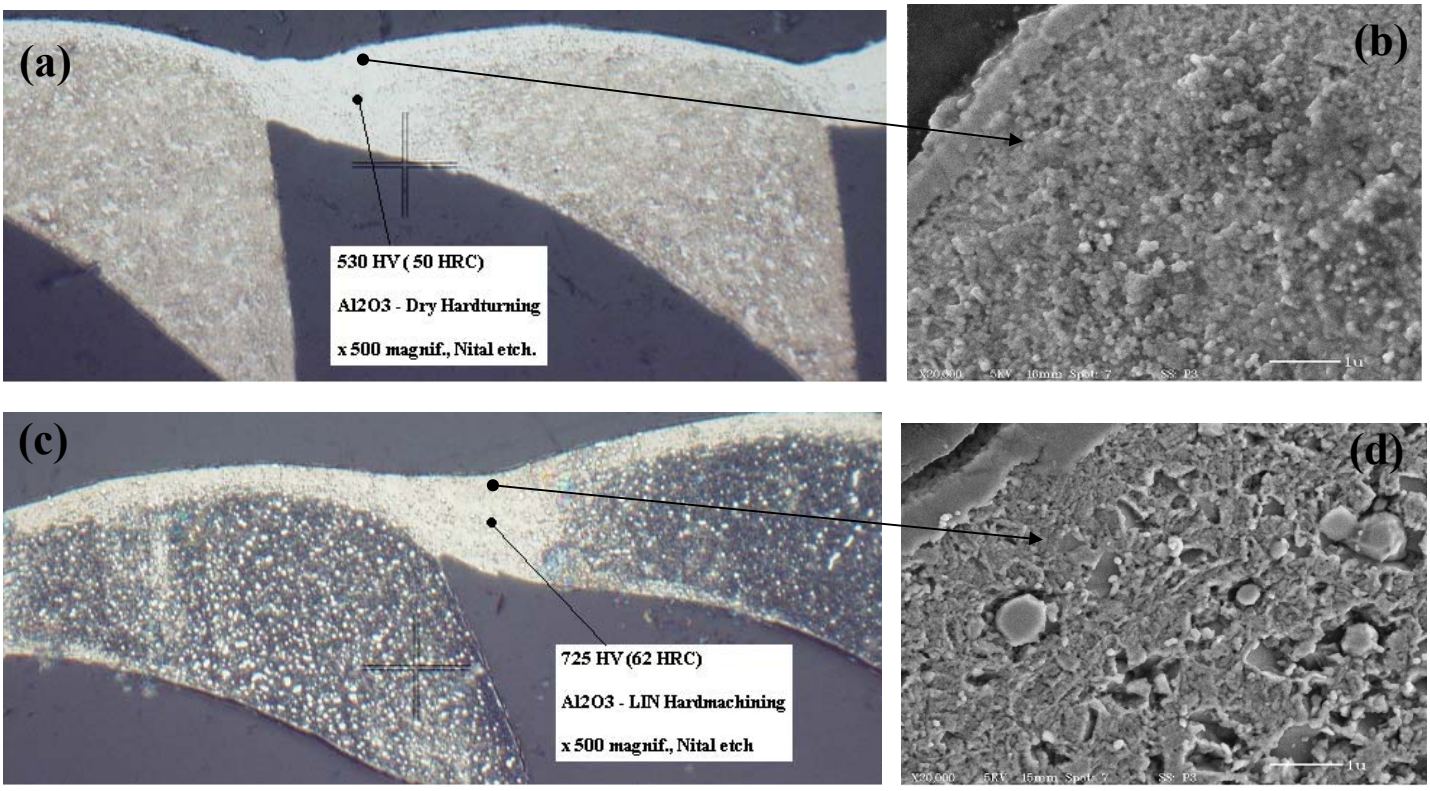

Fig.12: Random cross-section of a characteristically segmented 52100 chip, hard turned using the Al_2O_3 tool. (a - upper left) Optical metallography showing adjacent chip segments and inter-segment bridges produced during dry turning. (b - upper right) SEM close-up view of the bridge-tool interface area shown in (a), orig. magnif. x 20,000. (c – bottom left) Optical metallography showing adjacent chip segments and inter-segment bridges produced during LIN turning. (d – bottom right) SEM close-up view of the bridge-tool interface area shown in (c), orig. magnif. x 20,000.

The bulk of chip segments consists of a largely unaltered work material with tempered structure. Poorly etching in Nital, the segment bridges, along with the bridge-tool and the segment-tool interface layers, show an extensive microstructural change reminding of white layers formed on machined surface. High-magnification images of these white areas indicate a nanocrystalline, cell structure in the case of dry machining, and a submicron structure comprising carbides and ferrite in the case of LIN machining. The average cell size of the dry machined bridge is about 100 nm or 5-times more than in the case of white layer produced on the hard turned surface. This coarser white area structure, and the absence of dark areas of overtempered martensite, indicate that the affected chip material absorbed less of the thermo-mechanical energy than the machined work surface. The white bridge area of dry-machined chip is more refined and softer than the same area machined with LIN. The lower degree of structural refinement with LIN, and the retention of the initial hardness of the work material (62HRC) indicate that an effective removal of heat during hard turning can effectively reduce the extent of hard turning surface damage.

(*II*) As hard carbides dissolve in the hot, austenitic matrix of work surface, the material strength decreases to the point of unlocking a catastrophic shear. The mechanism of dissolution and strength loss is self-feeding as shown in Fig.14, since the melting point (solidus) of the steel decreases with increasing amount of carbon entering the matrix from dissolved carbides. The drop of strength with the decreasing melting point, i.e. increasing carbon, can be, conveniently, described with the Johnson-Cook constitutive law, eq. 1, [43-44] which clearly shows the critical effect of melting point on the flow stress of material. Thus, the width of the submicron-refined, localized shear band is a strong function of surface temperature. Also, the degree of structural refinement scales with temperature.

(*III*) A rapid cooling of the sheared layer with the tool departure results in 'freezing in-place' of the submicron, white layer structure. Small areas of unquenched martensite and retained austenite may develop within or just below the shared layer, above the dark layer of

an overtempered martensite, depending on the other parameters of the process.

Equation 1:

$$\sigma = (A + B\varepsilon^{n})\{1 + C\log(\frac{\dot{\varepsilon}}{\dot{\varepsilon}_0})\}\{1 - (\frac{T - 293}{T_{mp} - 293})^{m}\}$$

where:

σ is flow stress and ε is plastic strain,

$\dot{\varepsilon}$ and $\dot{\varepsilon}_0$ are strain rate and ref. strain rate, respectively,

T is temperature in Kelvin and T_{mp} is material melting point,

A, B, n, and m are material/microstructure sensitive constants with m values usually exceeding 1.0 for hardturned steels.

Reported carbon enrichment of the white layer's matrix [23] and localized thermal excursions to more than 1200°C [13] support the 3-step model proposed here and contradict the earlier observations of the constant carbon profile [7] or the retention of the original, tempering carbides within white layer [16-17].

Nanocrystalline ferritic/austenitic cell structures with extremely fine carbides, similar to the presently observed, were recently identified in white layers and chips using electron microscopy [45-46]. Beyond the machining technology field, the formation of load-induced nanostructures and white layers, combined with the dissolution of carbides were observed in the adiabatic processes of rolling and ball milling of ferritic steels [47], during service of high-speed train rails [48], and in shock- forming operations [49].

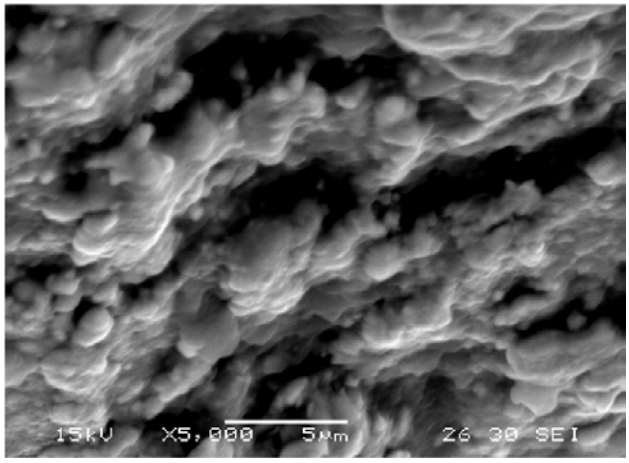

Fig.13: Surface detail of the Al_2O_3-TiCN cutting insert after dry hard turning at 700 ft/min (213 m/min) – chamfered land area located just above the undeformed chip imprint on tool, SEM, orig. magnif. x 5,000. Rounding of ceramic particles indicates an extensive surface diffusion or melting activated by high temperatures and/or interfacial, eutectic reactions with chip material. An ultrasonic acid bath cleaning of insert was used before SEM examination.

Consistent with the proposed physical model, the absence of white layer during hard turning of A2 steel can be explained by its higher degree of alloying, i.e. more thermally stable carbides that resist the dissolution and initiation of catastrophic shear. One can also infer, that heat treatments leading to coarser carbides may limit the thickness of hard turning white layers. Presented data indicates that the cryogenic, LIN-spray cooling effectively reduces the thickness of white layer by affecting the first two steps of material evolution – it reduces the temperature of cutting tool (conductive cooling), and cools the work surface around and behind the contact area (convective cooling).

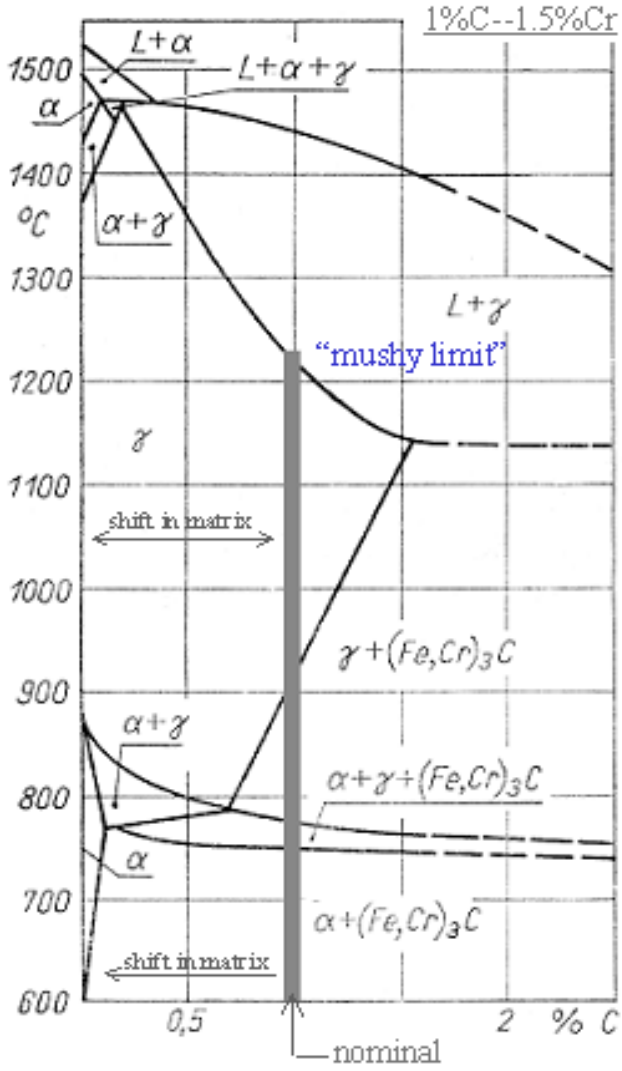

Fig.14: Fe-C cross-section through the ternary phase diagram of 1.5wt%Cr bearing steels [49]; the nominal composition of the AISI 52100 steel superimposed on the diagram indicates that with the dissolution of carbides in austenitic matrix, the incipient melting point (at solidus) drops to the temperature of just above 1200°C.

CONCLUSIONS

1. Cryogenic nitrogen spray cooling of cutting tool and tool-work contact area has been shown to effectively limit the thickness of white and dark layers, prevent softening of work surface and improve distribution of residual stresses.

2. Finish-hard turning with cryogenically cooled, inexpensive Al_2O_3 ceramic tools results in a thinner and more acceptable white layer (from an engineering property standpoint) than the conventional, dry CBN hard turning operation.

3. Compositional microanalysis and post-hard turning heat treatments indicate the absence of detectable reactions products at the machined surface that would point to the environmental or tool reaction effects on white layer.

4. A sequence of steps and conditions controlling white layer development were proposed based on experimental data including the observed nanostructure formation and an extensive dissolution of less-alloyed carbides. Of interest, the nanostructural refinement of white, shear layers is inversely proportional to work material temperature and cooling.

ACKNOWLEDGEMENTS

The authors would like to acknowledge Carl W. Zvanut and Dave R. Ruprecht of Air Products for encouragement and support, Lance M. Grimm for generating machining data, and John L. Green with Jim R. Stets for metallographic work and electron microscopy.

REFERENCES

[1] Brinksmeier, E., et al., 1982, "Residual Stresses – Measurement and Causes in Machining Processes"< Annals of the CIRP, Vol. 31/2, pp. 491-510

[2] Johnson, G.A., 1986, "Beneficial Compressive Residual Stress Resulting from CBN Grinding", Int. Grinding Conf., June 10-12, 1986, Philadelphia, Pennsylvania, SME Technical Paper MR86-625

[3] Shaw, M.C., 1994, "Heat-Affected Zones in Grinding Steel", Annals of the CIRP, Vol. 43/1, pp. 279-282

[4] Brinkmeier, E., 1992, "Hard Machining of Roll Components", Harterei-Technische Mitteilungen, 47(5), pp. 311-317

[5] Konig, W, et al., 1993, "Turning versus Grinding – A Comparison of Surface Integrity Aspects and Attainable Accuracies", Annals of the CIRS, Vol. 42/1, pp. 39-43

[6] Berktold, A., et al., 1994, "Top-Quality Components Not Only By Grinding", IDR 3/94, pp. 127-132

[7] Tonshoff, H.K., et al., 1995, "Potential and Limitation of Hard Turning", 1st Int. Machining and Grinding Conf., Sept. 12-14, 1995, Dearborn, Michigan, SME Technical Paper MR95-215

[8] Chou, Y-S., and Barash, M.M., 1995, "Review on Hard Turning and CBN Cutting Tools", *ibid*, SME Technical Paper MR95-214

[9] Packeisen, A., and Theisen, W., 1999, "Turning and Grinding of Hard Alloys", Advanced Engineering Materials, 1, No.1, pp. 35-48

[10] Matsumoto, Y., et al., 1999, "Surface Integrity Generated by Precision Hard Turning", Annals of the CIRP, Vol. 48/1, pp. 59-62

[11] Agha, S.R., and Liu, C.R., 2000, "Experimental study on the performance of superfinish hard turned surfaces in rolling contact", Wear 244, pp. 52-59

[12] Brockhoff, T., 1998, "Surface Hardening by Using Advanced Grinding Technology – A Paradigm Shift in Production Engineering", Abrasives, December/January, pp. 10-37

[13] Chou, Y.K., 2002, "Surface hardening of AISI 4340 steel by machining: a preliminary investigation", J. of Materials Processing Technology 124, pp. 171-177

[14] Fleming, M.A., et al., 1998, "PCBN hard turning and workpiece surface integrity", Industrial Diamond Review, 4/98, pp. 128-133

[16] Chou, Y.K., and Evans, C.J., 1998, "Process Effects on White Layer Formation in Hard Turning", Trans. Of NAMRI/SME, Vol. XXVI, pp. 117-122

[17] Chou, Y.K., and Evans, C.J., 1999, "White layers and thermal modeling of hard turned surfaces", Int. J. of Machine Tools & Manufacture 39, pp. 1863-1881

[18] Thiele, J.D., et al., 2000, "Effect of Cutting-Edge Geometry and Workpiece Hardness on Surface Residual Stresses in Finish Hard Turning of AISI 52100 Steel", Trans. Of ASME, Vol. 122, November 2000, pp. 642-649

[19] Thiele, J.D., and Melkote, S.N., 2000, "Effect of Tool Edge Geometry on Workpiece Subsurface Deformation and Through-Thickness Residual Stresses for Hard Turning of AISI 52100 Steel", J. of Manufacturing Processes, SME, Vol.2/No.4

[20] Chou, Y.K., and Song, H., 2001, "Hard Turning with Different Nose-Radius Ceramic Tools", 4th Int. Machining and Grinding Conf., May 7-10, 2001, Troy, Michigan, SME Technical Paper MR01-228

[21] Bahre, D., et al., 1998, "Modeling of Thermo-Elastic Workpiece Deformation for Compensation of Dimensional Errors in Turning of Hard Metals", Trans. Of NAMRI/SME, Vol. XXVI, pp. 123-128

[22] Broskea, T.J., 2000, "PCBN Tool Failure Mode Analysis", Intertech 2000, Vancouver, B.C., Canada, July 17-21, 2000

[23] Park, Y-W., 1999, "The Quantification of the Depth of Deformed Layer Using Elemental Analysis for Aspheric Lens Mold Core", Session 235, Proc. of the 3rd Int. Machining and Grinding Conf., October 4-7, 1999, Cincinnati, Ohio, pp. 243-251

[24] Dawson T.G., and Kurfess, T.R., 2001, "Tool Life, Wear Rates, and Surface Quality in Hard Turning", Trans. Of NAMRI/SME, Vol. XXIX, pp. 175-182

[25] Konig, W., et al., 1990, "Machining Hard Materials with Geometrically Defined Cutting Edges – Field of Applications and Limitations", Annals of the CIRP, Vol. 57, pp. 61-64

[26] Chou, Y.K., and Evans, C.J., 1997, "Finish Hard Turning of Powder Metallurgy M50 Steel", Trans. Of NAMRI/SME, Vol. XXV, pp. 81-86

[27] Mehrotra, P.K., 1998, “Applications of Ceramic Cutting Tools”, Key Engineering Materials, Vol. 138-140 (1998), chapter 1, pp. 1-24

[28] Zurecki, Z., and Harriott, G., 1998, “Industrial Systems for Cost Effective Machining of Metals Using an Environmentally Friendly Liquid Nitrogen Coolant”, Proc. of the Aerospace Manufacturing Technology Conf., SAE, Long Beach, CA, June 2-4,

[29] Zurecki, Z., et al., 1999, “Dry machining of metals with liquid nitrogen”, Proc. of the 3rd International Machining and Grinding ’99 Conf. and Expo, SME, Cincinnati, OH, October 4-7

[30] Rajurkar, K.P. and Wang, Z.Y., 1996, "Beyond Cool", Cutting Tool Engineering, Sept.1996, pp. 52-58

[31] Wang, Z.Y., et al., 1996, "Turning Ti-6Al-4V Alloy with Cryogenic Cooling", Trans. of NAMRI/SME, Vol. XXIV, pp. 3-8

[32] Wang, Z.Y., et al., 1996, "Cryogenic PCBN turning of ceramic (Si_3N_4)", Wear, Vol. 195 (1-2), pp. 1-6

[33] Wang, Z.Y., and Rajurkar, K.P., 1997, "Wear of CBN tool in turning of silicon nitride with cryogenic cooling", Int. J. of Machine Tools & Manufacture, Vol. 37, N. 3, Mar.1997, pp. 319-326

[34] Wang, Z. Y., and Rajurkar, K. P., 2000, “Cryogenic machining of hard-to-cut materials”, Wear, 239(2), pp. 168-175

[35] Hong, S.Y., and Broomer, M. ,2000, “Economical and ecological cryogenic machining of AISI 304 austenitic stainless steel”, Clean Products and Processes 2 (2000) 157-166, Springer-Verlag

[36] Hong, S.Y., et al., 2001, “New cooling approach and tool life improvement in cryogenic machining of titanium alloy Ti-6Al-4V”, Int. J. of Machine Tools and Manufacture, Vol. 41, Issue 15, Dec-2001, pp 2245-2260

[37] Hong, S.Y., and Ding, Y., 2001, “Cooling approaches and cutting temperatures in cryogenic machining of Ti-6Al-4V”, Int. J. of Machine Tools & Manufacture (2001) 41, (10), 1417-1437

[38] Dhar, N.R. et al., 2001, “The influence of cryogenic cooling on tool wear, dimensional accuracy and surface finish in turning AISI 1040 and E4340C steels”, Wear, 249(10-11), 932-942

[39] Paul, S., et al., 2001, “Beneficial effects of cryogenic cooling over dry and wet machining on tool wear and surface finish in turning AISI 1060 steel”, J. of Materials Processing Technology (2001) 116, (1), pp. 44-48

[40] Dhar, N.R., et al., 2002, “The effect of cryomachining cooling on chips and cutting forces in turning AISI 1040 and AISI 4320 steels”, Proc. Instn. Mech. Engrs., Vol. 216 Part B: J. Engineering Manufacture, ImechE 2002, pp. 713-724

[41] Ghosh, R., et al., 2003, “Cryogenic Machining with Brittle Tools and Effects on Tool Life”, paper no. IMECE2003-42232, to be published at the 2003 ASME Int. Mechanical Engineering Congress & Expo., Washington D.C., November 16-21, 2003

[42] Xingzhong, Z., et al., 1997, “Wear mechanisms of Ti(C,N) ceramic in sliding contact with stainless steel”, J. of Materials Sci., 32, pp. 2963-2968

[43] Becze, C.E., et al., 2001, “High Strain Rate Shear Evaluation and Characterization of AISI D2 Tool Steel in Its Hardened State”, Machining Sci. and Technology, 5 (1), pp. 131-149

[44] Ng, E-G, et al., 2002, “Physics-Based Simulation of High Speed Machining”, Machining Sci. and Technology, Vol. 6, No. 3, pp. 301-329

[45] Barry, J., and Byrne, G., 2002, “Chip Formation, Acoustic Emission and Surface White Layers in Hard Machining”, Annals of the CIRP, Vol. 51/1/2002, pp. 65-70

[46] Barbacki, A., et al., 2003, “Turning and grinding as a source of microstructural changes in the surface layer of hardened steel”, J. of Materials Processing Technology 133 (2003) 21-25

[47] Umemoto, M., et al., 2001, “Formation of Nanocrystalline Ferrite through Rolling and Ball Milling”, Material Sci. Forum Vols. 360-362, pp. 167-174

[48] M. Djahanbakhsh, M., et al., 2001, “Nanostructure Formation and Mechanical Alloying in the Wheel/Rail Contact Area of High Speed Trains in Comparison with Other Synthesis Routes”, J. of Metastable and Nanocrystalline Materials, Mat. Sci. Forum Vols. 360-362, pp. 175-182

[49] Atroshenko, S.A., 2001, “Shock Induced Nanocrystalline Formations in Metals”, Proc. of the 22nd Riso Int. Symposium on Materials Science: Science of Metastable and Nanocrystalline Allos Structure, Properties and Modeling, Ed. Dinesen, A.R., et al., Riso National Laboratory, Roskilde, Denmark 2001, pp. 193-198

[49] Luty, W., 1980, “Physical Metallurgy and Heat Treatment of Bearing Steels”, Wydawnictwo Naukowo-Techniczne, Warsaw, ISBN 83-204-0169-0, p. 58